Carbohydrate Polymers 92 (2013) 856–864

Contents lists available at SciVerse ScienceDirect

Carbohydrate Polymers

journal homepage: www.elsevier.com/locate/carbpol

Self-assembled nanoparticles of modified-chitosan conjugates for the sustained release of DL-α-tocopherol

Javier Pérez Quiñones[a,*], Kurt Vesterager Gothelf[b], Jørgen Kjems[c], Chuanxu Yang[c], Angeles María Heras Caballero[d], Claudia Schmidt[e], Carlos Peniche Covas[f]

[a] Center of Natural Products, Faculty of Chemistry, University of Havana, Havana, Cuba
[b] Interdisciplinary Nanoscience Center (iNANO)/Department of Chemistry, Aarhus University, Aarhus, Denmark
[c] Interdisciplinary Nanoscience Center (iNANO)/Department of Molecular Biology, Aarhus University, Aarhus, Denmark
[d] Instituto de Estudios Biofuncionales/Dpto Química Física II, Facultad de Farmacia, Universidad Complutense de Madrid, Spain
[e] Department of Chemistry, University of Paderborn, Paderborn, Germany
[f] Center of Biomaterials, University of Havana, Havana, Cuba

ARTICLE INFO

Article history:
Received 29 August 2012
Received in revised form 4 October 2012
Accepted 4 October 2012
Available online 13 October 2012

Keywords:
Chitosan conjugates
Controlled release
Self-assembled nanoparticles
Tocopherol

ABSTRACT

Synthetic O6-succinylated chitosan and commercial glycol chitosan were covalently linked to DL-α-tocopheryl monoesters for controlled release of vitamin E. These conjugates formed self-assembled nanoparticles in aqueous solution with 254–496 nm mean diameters and DL-α-tocopherol contents between 27 and 39% (w/w). The particles appeared as 40–75 nm almost spherical nanoparticles when studied by scanning and transmission electron microscopy upon drying. Drug linking to chitosan matrix was confirmed by FTIR spectroscopy and proton NMR. Conjugates were also characterized by differential scanning calorimetry and wide-angle X-ray diffraction. *In vitro* tocopherol release studies performed in water at acid pH indicated a drug release dependence on drug content, hydrated particle sizes and employed chitosan derivative. Almost constant release rates were observed the first 7 h. The obtained nanoparticles exhibited radical scavenging activity in DPPH essay. The potential of these nanoparticles was also demonstrated by the enhancement of HMVEC cell proliferation.

1. Introduction

Vitamin E (with α-tocopherol as the most studied and bioavailable component) is a lipophilic compound mainly found in biomembranes (Brigelius-Flohé & Traber, 1999). Its phenolic hydroxyl group donates hydrogen atoms, working as a cell membrane protecting agent and as a free radical scavenger involved in the lipid peroxidation chain reactions (Atkinson & Traber, 2007; Bongiorno et al., 2006). It also protects fats and low-density lipoproteins (LDLs) from oxidation. Antioxidant, anticancer, anti-inflammatory and cardiovascular-protective activities associated with α-tocopherol has been widely studied (Buring, Glynn, Goldhaber, Ridker, & Zee, 2007; Christen, Jiang, & Reiter, 2007). Several drug delivery systems have been prepared releasing or including tocopherol or tocopherol derivatives in their formulations (Basaran, Yazan, & Yenilmez, 2010; Liu & Park, 2009). However, the design of proper dosage forms is still challenging due to its hydrophobicity and well-known sensitivity to oxygen and light (Duclairoir, 2002; Lodge, 2005).

Chitosan is a biopolymer obtained by extensive deacetylation of chitin, the second most abundant polysaccharide in nature and essential component of arthropods, insects, molluscs and crustacean exoskeletons and the cell walls of fungi (Muzzarelli, 2009). Isolated chitosan is the linear and partly acetylated (1–4)-2-amino-2-deoxy-β-D-glucan. Chitosan is preferred over chitin for medical and technical use because it can be dissolved in dilute acid solutions and can be casted into films or prepared as membranes, microspheres and nanoparticles (Ravi Kumar, Muzzarelli, Muzzarelli, Sashiwa, & Domb, 2004). Furthermore, chitosan is considered an excellent biomaterial (biocompatible, biodegradable and nontoxic) with mucoadhesive, antifungal and bactericide properties (Acosta, Heras, & Paños, 2008; Kean & Thanou, 2010; Muzzarelli et al., 2012). The antioxidant and hypocholestemic properties of chitosan are also well known and exploited in formulations encapsulating vitamin E for drug delivery systems (Amir et al., 2010; Basaran et al., 2010). However, the limited water solubility and precipitation of self-aggregated chitosan conjugates, restricts its application in medical practice (Babak et al., 2007). In contrast, glycol chitosan exhibits a good water solubility at all pHs, biocompatibility and is widely applied as hydrophobic drug and gene carrier (Cho et al., 2006). In this sense, our group synthesized glycol chitosan hydrophobically-modified with ergocalciferol hemisuccinate

* Corresponding author. Tel.: +53 7 870 2102.
E-mail addresses: javierp@fq.uh.cu, javenator@gmail.com (J.P. Quiñones).

0144-8617/$ – see front matter © 2012 Elsevier Ltd. All rights reserved.
http://dx.doi.org/10.1016/j.carbpol.2012.10.005

for controlled release of vitamin D2 (Quiñones et al., 2012). However, to our knowledge the preparation of covalently linked tocopherol–glycol chitosan nanoparticles for controlled release of vitamin E has not been reported.

The aim of this work was to prepare self-assembled nanoparticles of soluble chitosan derivatives (O6-succinylated chitosan and glycol chitosan) conjugated to vitamin E in order to accomplish the controlled release of the drug and to combine the antioxidant effects of DL-α-tocopherol with the microbicidal properties of chitosan (Anraku et al., 2011).

2. Materials and methods

2.1. Materials

Chitosan (acetylation degree, DA = 14.8%, determined by ^{1}H NMR, $M_W = 2.55 \times 10^5$) was obtained by extensive deacetylation of chitin isolated from shells of common lobster (*Panulirus argus*) at the Center of Biomaterials of the University of Havana, Cuba. Glycol chitosan (acetylation degree, DA = 19.1%, determined by ^{1}H NMR, $M_W = 4.1 \times 10^5$) was purchased from Sigma–Aldrich. Vitamin E monoesters were synthesized by base-catalyzed traditional esterification in pyridine of DL-α-tocopherol with succinic, maleic and itaconic anhydrides, respectively (Abe, Hasunuma, & Kurokawa, 1976). Partially O6-succinylated chitosan was obtained by direct esterification with succinic anhydride of N-phtaloyl chitosan (prepared from aforementioned chitosan) and subsequent deprotection (N-phtaloyl removal) with hydrazine monohydrate (Fang & Huang, 2006; Shen, Ping, Zhang, & Zhang, 2003). The vitamin E (DL-α-tocopherol), DDPH (1,1′-diphenyl-2-picrylhydrazyl), Trolox ((±)-6-hydroxy-2,5,7,8-tetramethylchromane-2-carboxylic acid), solvents and reagents employed were purchased from Sigma–Aldrich and used without further purification.

The structures of vitamin E monoesters: DL-α-tocopheryl hemisuccinate (MST), DL-α-tocopheryl monoitaconate (MIT), DL-α-tocopheryl monomaleate (MMT), O6-succinylated chitosan (SCS), glycol chitosan (GC) and schematic illustrations of hydrophobically-modified chitosan nanoparticles with tocopheryl hydrophobic core and external hydrophilic chitosan moiety are shown in Fig. 1.

2.1.1. Synthesis of N-tocopheryl glycol chitosans and N-tocopheryl O6-succinylated chitosan conjugates

130 mg (0.61 mmol) of glycol chitosan or O6-succinylated chitosan was dissolved in 8 mL of double-distilled water and diluted with 24 mL of anhydrous ethanol. Then 38 mg (0.20 mmol) of 1-ethyl-3-(3′-dimethylaminopropyl)carbodiimide hydrochloride and 23 mg (0.20 mmol) of N-hydroxisuccinimide were added and stirred until solution clearance. 80 mg (c.a. 0.15 mmol) of DL-α-tocopheryl monoesters were dissolved in 32 mL of ethanol/water solution (85:15, v/v) and slowly added with stirring to the chitosans solution. The reaction mixture was stirred at room temperature 72 h, dialyzed against ethanol/water solution (90:10, 66:33, 50:50 and 0:100, v/v), each one for 2 days with 16 exchanges. These dialyzed solutions were freeze-dried affording white or yellow, cotton wool-like products.

2.1.2. Preparation of the self-assembled nanoparticles

The synthesized N-tocopheryl glycol chitosans and N-tocopheryl O6-succinylated chitosan were able to form nanoparticles on aqueous solution after stirring overnight and probe tip sonication. To this end, the modified-chitosan conjugates (c.a. 0.5–2.0 mg mL^{-1}) were stirred overnight at 100 rpm on double-distilled water or phosphate-buffered saline (PBS) solution, as required. The solutions were probe tip sonicated (Branson Sonifier W-250, Heinemann, Germany) at 20 W for 2 min on an ice bath. The sonication step was repeated five times. The pulse function was pulsed on 8.0 s and pulsed off 2.0 s (Jing-Mou, Li-Yan, Yi, & Yong-Jie, 2008).

2.2. Characterization

2.2.1. Characterization of N-tocopheryl glycol chitosans and O6-succinylated chitosan conjugates

The N-tocopheryl glycol chitosans and O6-succinylated chitosan conjugates were characterized by FTIR spectroscopy using a Perkin-Elmer 1720 FTIR spectrophotometer with 32 scans and 4 cm^{-1} resolution. Samples were prepared by the KBr pellet method. Elemental analyses were performed on a Vario MicroCube Analyzer with burning temperature of 1150 °C. The ^{1}H NMR spectra were recorded with a VARIAN Oxford AS400 NMR spectrometer operating at 400.46 MHz for ^{1}H at 25 °C with concentrations c.a. 25–8 mg mL^{-1} in d2-water and d4-methanol/d2-water (66%, v/v) and analyzed with the VNMRJ software, version 2.2 (Berrada et al., 2003; Jing-Mou et al., 2008). Wide-angle X-ray diffraction of the powered samples was performed using a Rigaku SmartLab X-Ray diffractometer with Cu Kα radiation (40 kV, 180 mA, λ = 0.15418 nm), data collected at a scan rate of 5° min^{-1} with a scan angle from 4 to 50°. Calorimetric curves were obtained with a Perkin-Elmer Differential Scanning Calorimeter Pyris 1 and analyzed with the Pyris 1 software (version 6.0.0.033). DSC studies were conducted using sample weights of approximately 5 mg, under a nitrogen dynamic flow of 20.0 mL min^{-1} and a heating-cooling rate of 10 °C min^{-1} (Basaran et al., 2010). Samples were deposited in aluminum capsules and hermetically sealed. Indium was used to calibrate the instrument. Enthalpy (ΔH in J/g dry weight) and peak temperature were computed automatically. Samples were heated and cooled from −30 to 300 °C.

2.2.2. Characterization of nanoparticles

Dynamic light scattering (DLS) studies were performed using Zetasizer Nano ZS (Malvern Instruments, Malvern, UK) at 25 °C to obtain the particle size and zeta potential. For zeta potential measurements nanoparticles were prepared in double-distilled water (c.a. 1–2 mg mL^{-1}), while particle size measurements were conducted on PBS solution (c.a. 0.5–1 mg mL^{-1}). The size and morphology of dried nanoparticles were studied by transmission electron microscopy (TEM) with a Philips CM20 operating at 200 kV and scanning electron microscopy (SEM) with a Nova NanoSEM 600 electron microscope. Each sample was stirred 48 h in double-distilled water (c.a. 1 mg mL^{-1}), probe tip sonicated as already described and a drop of it was deposited on carbon plates. The excess solution was removed with filter paper and air-dried. The SEM samples were sputter-coated with gold. The TEM samples were negative stained with uranyl acetate solution (1%).

2.3. In vitro drug release studies

In vitro vitamin E release from N-tocopheryl glycol chitosans and O6-succinylated chitosan nanoparticles was studied by UV detection (Genesys 10 UV–vis spectrophotometer) at 292 nm of the delivered DL-α-tocopherol at pH 6. 10–15 mg of tocopheryl-modified nanoparticles dissolved in PBS solution at pH 6 (5 mL) were placed in dialysis bags and dialyzed against the release media (PBS, pH 6.0, 40 mL) at 37 °C with constant agitation at 100 rpm. The entire media were removed at determined time intervals, and replaced with the same volume of fresh media. The amount of DL-α-tocopherol released was determined by UV spectrophotometry and calculated from a previously obtained calibration

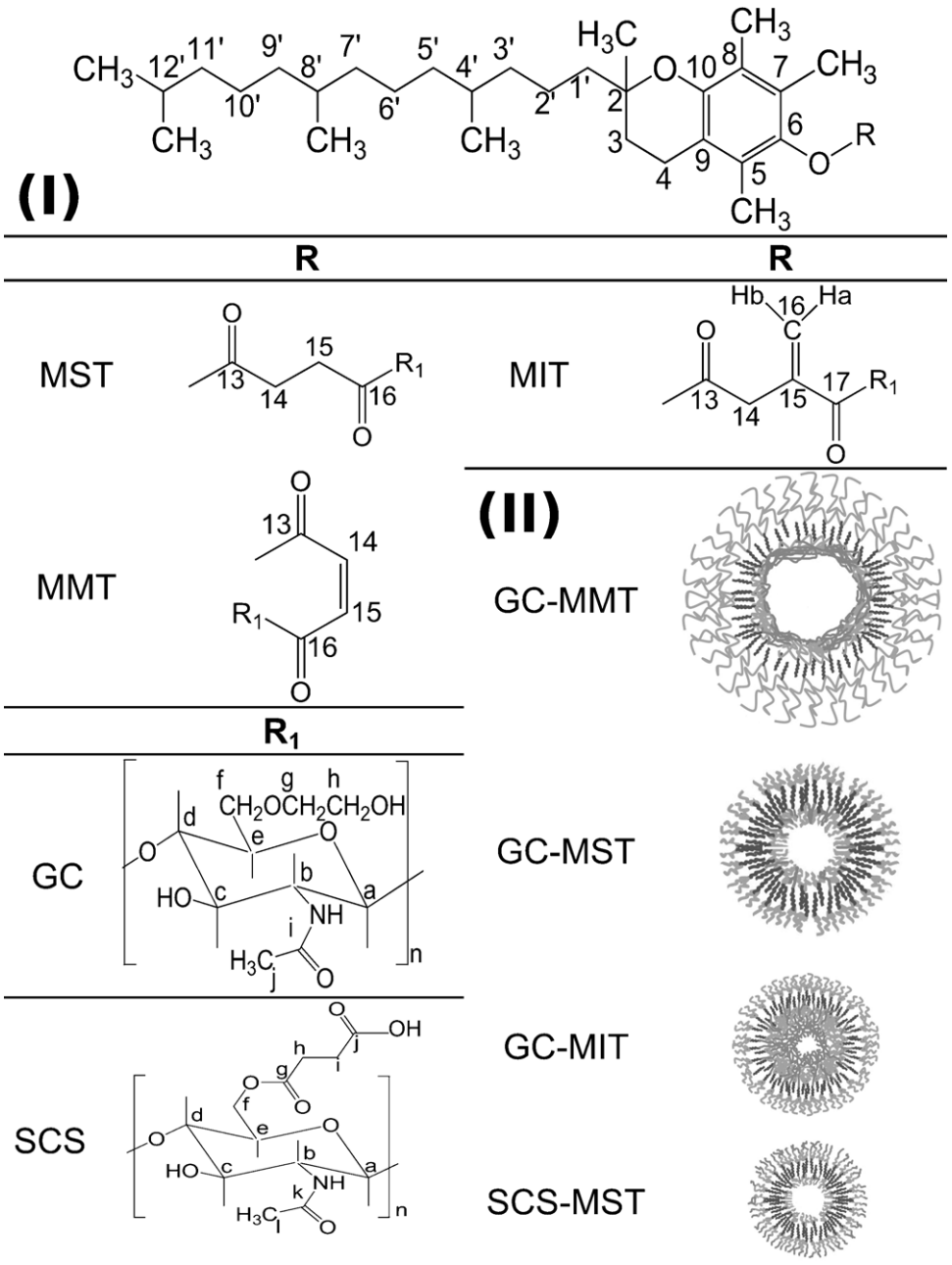

Fig. 1. (I): Structure of DL-α-tocopheryl monoesters (MST, MIT, MMT), O6-succinylated chitosan (SCS) and glycol chitosan (GC); (II) schematic illustration of modified-chitosan nanoparticles with tocopheryl hydrophobic core and external hydrophilic chitosan moiety.

curve. These studies were conducted in triplicate for each sample.

2.4. Biological activity bioassays

2.4.1. In vitro antioxidant activity

The antioxidant activity of the obtained tocopheryl-modified chitosan nanoparticles was evaluated trough the *in vitro* test of DPPH (1,1′-diphenyl-2-picrylhydrazyl) and compared with similar concentrations of Trolox ((±)-6-hydroxy-2,5,7,8-tetramethylchromane-2-carboxylic acid) (Anraku et al., 2011; Basaran et al., 2010). Briefly, 0.2 mL of ethanol and 0.3 mL of the release media (or same molar concentration of Trolox) at different time intervals were mixed in a 10 mL eppendorf tube, subsequent DPPH (2.5 mL of 75 μM in ethanol) was added. The solution was kept in darkness at room temperature 30 min and the absorbance at λ = 517 nm (A_{517}) was measured. The radical scavenging effect was calculated as:

$$\%\ \text{radical scavenging effect} = \frac{A_0 - A_{517}}{A_0} \times 100$$

where A_0 is the absorbance of blank DPPH at 517 nm. No corrections were needed to A_{517} because the samples were transparent at this wavelength.

2.4.2. Cell culture and cytotoxicity

MCF-7 cells (human breast adenocarcinoma cell line) were maintained in DMEM (Invitrogen) media supplemented with 10% fetal bovine serum, 1% penicillin–streptomycin at 37 °C in 5% CO_2 and 100% humidity. Human Microvascular Endothelial Cells (HMVEC) were cultured in Endothelial Cell Basal Medium-2 (Lonza)

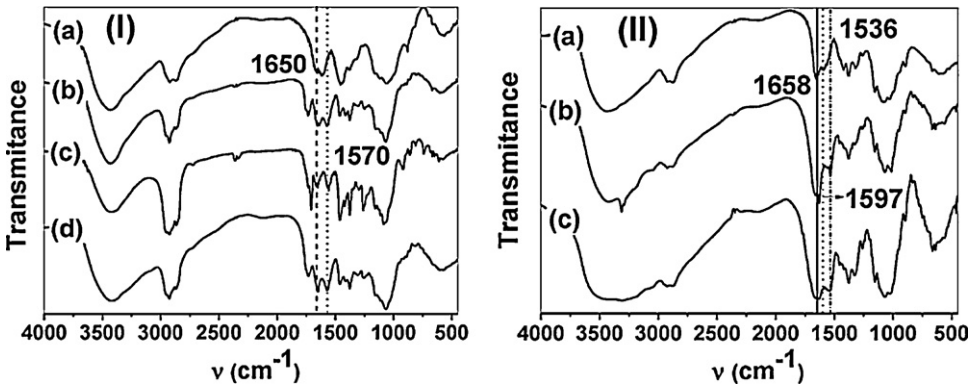

Fig. 2. Infrared spectra of (I): (a) GC, (b) GC-MST, (c) GC-MIT, (d) GC-MMT; (II): (a) CS, (b) SCS and (c) SCS-MST (see Fig. 1 for structures).

supplemented with EGM-2 singlequots (Lonza) containing h-EGF, VEGF, h-FGF-B, R3-IGF-1, hydrocortisone, and FBS (2% final concentration).

Cytotoxicity of all the samples was tested on both MCF-7 and HMVEC cells by MTS assay (CellTiter 96® Aqueous One Solution Reagent). H1299 and HeLa cells in full growth media were seeded in 96-well plate (1×10^4 cells/well). After the cells attached on the plate, the media was changed to serum free media and vitamin E and tocopheryl-modified chitosan conjugates with different concentration were added. After incubation for 48 h, the media was replaced with full growth media, 20 μL MTS reagent was added to each well and incubated for additional 3 h before measuring the absorbance at 490 nm using a 96-well plate reader (μQuant, Bio-Tek Instruments Inc., USA).

3. Results and discussion

The employed method afforded N-tocopheryl glycol chitosan and O6-succinylated chitosan conjugates with substitution degrees of up to 22.8 mol% (GC-MST), 36.3 mol% (GC-MIT), 20.9 mol% (GC-MMT) and 16.2 mol% (SCS-MST); equivalent to DL-α-tocopherol weight contents of 29.7% (w/w) (GC-MST), 38.6% (w/w) (GC-MIT), 28.1% (w/w) (GC-MMT) and 27.6% (w/w) (SCS-MST), respectively. The higher vitamin E contents were obtained when the reaction was conducted with glycol chitosan. The general trend of observed α-tocopheryl monoesters reactivity with glycol chitosan was: MIT > MST∼MMT.

The obtained conjugates formed self-assembled nanoparticles in aqueous solution, due to their hydrophilic/hydrophobic moieties. The particles structure is affected by the media polarity, as observed in proton NMR peak differences in d2-water compared to d4-methanol/d2-water (66%, v/v).

The FTIR spectra of N-tocopheryl glycol chitosan conjugates are shown in Fig. 2(I). The spectrum of glycol chitosan is also included for comparison. Fig. 2(II) shows the spectra of chitosan, O6-succinylated chitosan and N-tocopheryl O6-succinylated chitosan.

The IR spectrum of glycol chitosan (Fig. 2(I), (a)), presented the characteristic absorption peaks at 3432 cm^{-1} (O—H stretching overlapped with N—H stretching), 2926 cm^{-1} and 2870 cm^{-1} (aliphatic C—H stretching band), 1650 cm^{-1} (amide I band, C=O stretching of acetyl group), 1616 cm^{-1} (N—H bending) and 1450–1380 cm^{-1} (C—H bending). The absorption peaks at 1160 cm^{-1} (antisymmetric stretching of the C—O—C bridge), 1120 and 1066 cm^{-1} (skeletal vibrations involving the C—O stretching) are due to its saccharide structure (Jing-Mou et al., 2008).

The spectra of N-tocopheryl glycol chitosan conjugates are dominated by the broad peaks of glycol chitosan; however the intense C=O peaks of the ester linkage are present at 1734 cm^{-1} (GC-MST), 1734 cm^{-1} (GC-MIT) and 1732 cm^{-1} (GC-MMT) (see Fig. 2(I), (b–d)). Intense peaks at 1570 cm^{-1} and the increase in the amide I band at 1650 cm^{-1} confirm the amide linkage between the glycol chitosan and tocopheryl monoesters (MST, MIT, MMT).

The IR spectrum of chitosan (Fig. 2(II), (a)) presented characteristic absorption peaks at 2942–2784 cm^{-1} (aliphatic C—H stretching band), 1658 cm^{-1} (Amide I), 1597 cm^{-1} (—NH_2 bending) and 1321 cm^{-1} (Amide III). Absorption peaks at 1154 cm^{-1} (antisymmetric stretching of the C—O—C bridge), 1082 and 1032 cm^{-1} (skeletal vibrations involving the C—O stretching) are due to its saccharide structure (Quiñones, Coll, Curiel, & Covas, 2010). The IR spectrum of O6-succinylated chitosan (Fig. 2(II), (b)) presents in addition to chitosan peaks, defined absorption at 1634 cm^{-1} (C=O peaks of ester linkage).

The IR spectrum of N-tocopheryl O6-succinylated chitosan conjugate is dominated by the intense and broad peaks of chitosan; but the C=O peak of ester linkage at 1639–1628 cm^{-1} are overlapping the Amide I and —NH_2 peaks at 1660–1652 cm^{-1} and 1597 cm^{-1}, producing a broad band ranging from 1700 to 1600 cm^{-1}. Also is observed an intense peak at 1538–1560 cm^{-1} and increase in the amide I band at 1658 cm^{-1}, as resulting of amide linkage between the O6-succinylated chitosan and tocopheryl hemisuccinate (MST).

The proton NMR spectra of N-tocopheryl glycol chitosan conjugates are shown in Fig. 3. The placebo glycol chitosan is also showed for comparison.

The ^1H NMR spectrum of glycol chitosan showed the characteristic signals of the saccharide protons at 2.09 ppm (s, C_jH_3 of partial acetylation, CH_3CO—), 2.74 ppm (s, 2 H, C_b sugar protons of N-unsubstituted glucosamine units), 3.2–4.0 ppm (C_c to C_h sugar protons) and 4.49 ppm (s, C_a anomeric sugar proton) (Gray et al., 2001; Gray, Noble, Sadiq, & Uchegbu, 1999). Compared with glycol chitosan, in the proton NMR spectrum of GC-MST (Fig. 3(I), (b)), the peaks at 0.91 ppm (CH_3, 4′-CH_3 + 8′-CH_3 + 12′-CH_3), 1.29 ppm (CH_3 + CH_2, 2-CH_3 + H1′ to H12′), 2.61 ppm (CH_2, H14 + H15 of succinyl moiety), 4.21 ppm and 4.54 ppm (CH, C_a anomeric sugar proton of tocopheryl substituted and free glycol chitosan respectively) are observed. Addition of d4-methanol to previously prepared d2-water solution of GC-MST, until a composition of d4-methanol/d2-water (66%, v/v), enhance the peak intensity in the proton NMR spectrum, due to a better solubility and amphiphilic behavior of N-tocopheryl glycol chitosan conjugates (Fig. 3(II), (a)).

The proton NMR spectra of GC-MIT in CD_3OD/D_2O (Fig. 3(II), (b)) also presents the characteristic tocopheryl peaks at 0.93 ppm (CH_3, 4′-CH_3 + 8′-CH_3 + 12′-CH_3), 1.25–1.39 ppm (CH_3 + CH_2, 2-CH_3 + H1′ to H12′), 2.27 ppm (CH_2, H14 of itaconyl moiety), 4.09 ppm (C_c to C_h sugar protons of glycol chitosan) and 4.23 ppm (CH, C_a anomeric sugar proton of tocopheryl substituted glycol chitosan). GC-MMT (Fig. 3(II), (c)) showed intense peaks at 0.81 ppm (CH_3,

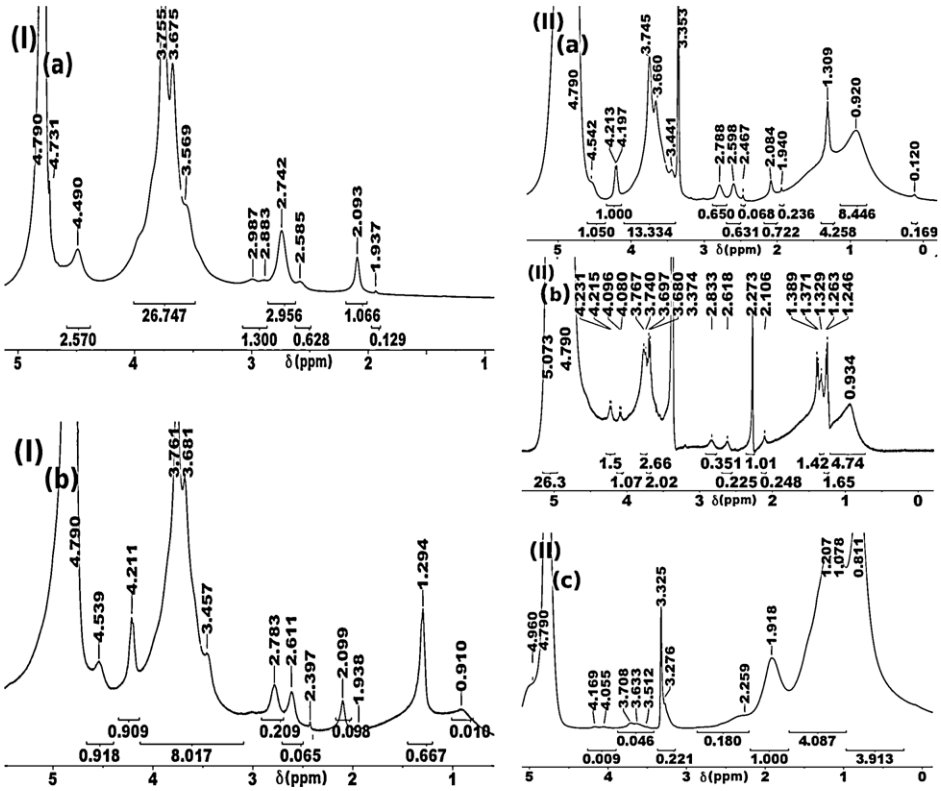

Fig. 3. Proton NMR spectra of (I): (a) GC, (b) GC-MST at 25 mg mL^{-1} in D_2O at 25 °C; (II): (a) GC-MST, (b) GC-MIT, (c) GC-MMT at 8 mg mL^{-1} in CD_3OD/D_2O (2:1) at 25 °C (see Fig. 1 for structures).

4′-CH_3 + 8′-CH_3 + 12′-CH_3), 1.21 ppm (CH_3 + CH_2, 2-CH_3 + H1′ to H12′), 1.92 ppm (CH_3, 5-CH_3 + 7-CH_3 + 8-CH_3) and 4.17 ppm (CH, C_a anomeric sugar proton of tocopheryl substituted glycol chitosan).

Proton NMR spectrum of chitosan (Fig. 4(a)) showed characteristic peaks at 2.10 ppm (s, CH_3 of partial acetylation, CH_3CO—), 3.19 ppm (s, 1H, H_b), 3.75 ppm (s, 1H, H_e), 3.80 ppm (s, 1H, $H_{f'}$) and 3.91 ppm (s, 3H, H_c + H_d + H_f) as reported for crab chitosans (Berrada et al., 2003; Hirai, Nakajima, & Odani, 1991). O6-Succinylated chitosan (Fig. 4(b)) presented, in addition to proton peaks of chitosan, signals at 2.74–2.95 ppm (CH_2, H_h + H_i of succinate group) and 7.3–8.4 ppm (C_8H_4, partially N-phtaloyled chitosan moiety). The proton NMR spectra of N-tocopheryl O6-succinylated chitosan (SCS-MST) (Fig. 4(c)), presented the intense chitosan peaks and additional peaks at 0.77–0.81 ppm (CH_3, 4′-CH_3 + 8′-CH_3 + 12′-CH_3), 1.21 ppm (CH_3 + CH_2, 2-CH_3 + H1′ to H12′), 2.49–2.97 ppm (CH_2, H14 + H15 + H_h + H_i of succinyl moieties), attributed to tocopheryl hemisuccinate moiety.

The wide-angle X-ray diffraction patterns of glycol chitosan, N-tocopheryl glycol chitosan conjugates, tocopheryl hemisuccinate, chitosan and N-tocopheryl O6-succinylated chitosan are shown in Fig. 5.

Glycol chitosan present broad an intense peaks at 2θ 7.7° and 20.1°.

N-tocopheryl glycol chitosan conjugates presents peaks at 2θ 4.0° and 2θ between 19.0 and 19.9°. The lack of intense peaks at 2θ 7.7° and 20.1° related to glycol chitosan is indicative of the absence of the unmodified-glycol chitosan crystalline phase.

Chitosan presented low crystallinity, but defined peaks at 2θ 10.7° and 20.0° are observed. These peaks are attributed to the $(0\,2\,0)_h$ planes of the hydrated crystalline structure and the reflections of the hydrated polymorph respectively (David et al., 2010). These defined peaks are also observed in chitosans from crab shells (Mau, Yang, & Yen, 2009). O6-Succinylated chitosan shows several intense peaks between 2θ 6.7° and 25.2°; but the characteristic chitosan peaks are absent.

N-tocopheryl O6-succinylated chitosan presented intense peaks at 2θ 4.0°, 10.6° and 19.9°. The characteristic peaks of O6-succinylated chitosan and pure tocopherol hemisuccinate were missing, as expected due to their absence as crystalline phase.

Glycol chitosan (Fig. 6(I), (a)) presents three endothermic peaks at 123.6 °C, 175.1 °C and 180.9 °C, with associated peak enthalpy (ΔH) of 81.9 J/g, 510.5 J/g and 72.1 J/g, respectively. N-Tocopheryl glycol chitosans (Fig. 6(I), (b)–(d)) showed several intense endothermic peaks at 205.0 °C, 208.9 °C, 263.0 °C and 268.1 °C (GC-MST), with related ΔH of 20.1 J/g, 27.2 J/g, 34.7 J/g and 83.8 J/g, respectively; 192.7 °C, 230.4 °C, 238.2 °C and 247.2 °C (GC-MIT), with related ΔH of 262.3 J/g, 281.1 J/g, 31.2 J/g and 193.2 J/g, respectively; 225.0 °C (GC-MMT), with related ΔH of 216.4 J/g. These peaks can result from the melting of glycol chitosan with linked tocopheryl monoesters, dissociation and decomposition of N-tocopheryl glycol chitosan chains.

The DSC of chitosan placebo (Fig. 6(II), (a)) showed two endothermic peaks at 170.4 °C and 187.0 °C, respectively. The total ΔH of these effects is 124.1 J/g. These endothermic effects must result mainly from the melting and dissociation of chitosan crystals, by comparison with reports for crab chitosans (Quiñones et al., 2010).

The DSC of O6-succinylated chitosan shows an intense peak at 175.0 °C with associated ΔH of 165.6 J/g (Fig. 6(II), (b)). N-Tocopheryl O6-succinylated chitosan (Fig. 6(II), (c)) showed two endothermic peaks at 202.0 °C and 272.8 °C, with associated peak enthalpies of 115.7 J/g and 375.3 J/g, respectively.

Dynamic light scattering studies conducted in triplicate afforded average particles diameters of 392 ± 8 nm with a polydispersity index (PDI) of 0.211 ± 0.006 (GC-MST), 284 ± 3 nm with PDI: 0.02 ± 0.01 (GC-MIT), 496 ± 5 nm with a PDI: 0.30 ± 0.08

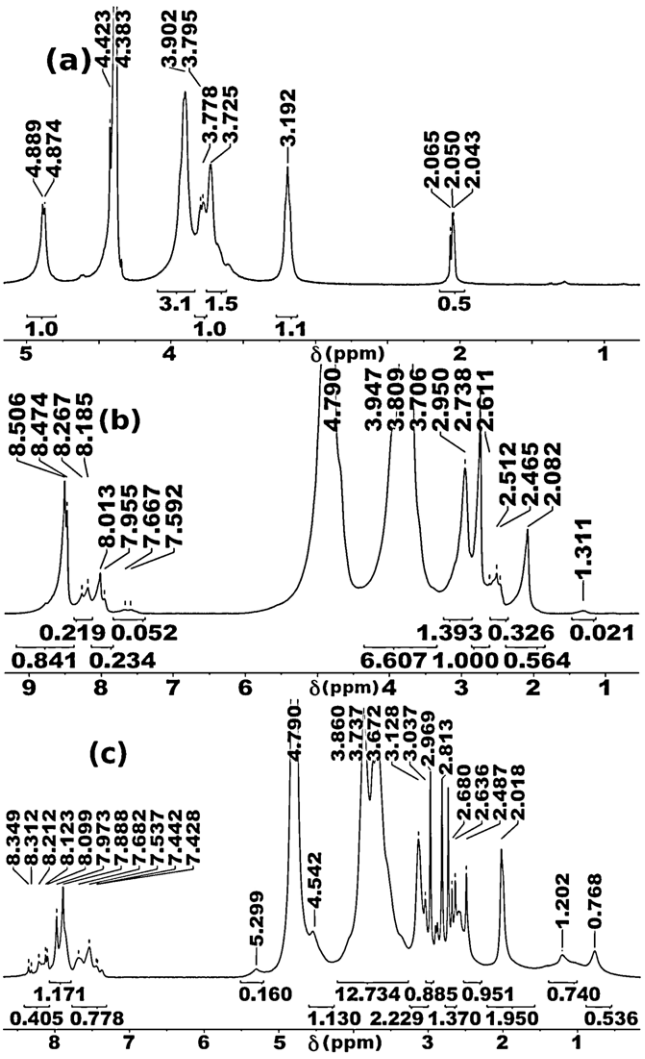

Fig. 4. Proton NMR spectra of (a) CS at 10 mg mL^{-1} in CD_3COOD/D_2O (1:3), (b) SCS and (c) SCS-MST at 15 mg mL^{-1} in D_2O at 25 °C (see Fig. 1 for structures).

(GC-MMT) and 254 ± 4 nm with a PDI of 0.25 ± 0.03 (SCS-MST). These nanoparticles were accompanied by c.a. 3–8 mol% aggregates of about 4.7–5.6 μm sizes. The hydrodynamic particle size of glycol chitosan conjugates in PBS solution seems to be mostly determined by the hydrophobic component and chain accommodation at molecular level on the hydrophobic core as schematically represented in Fig. 1. GC-MMT conjugate with the lower tocopheryl substitution degree and more steric constraint (C_{14}═C_{15} rigid structure, not linear) at MMT moiety presents a less compact hydrophobic core and bigger nanoparticle mean diameter; while GC-MST with a similar substitution degree is able to accommodate better the tocopheryl chains (free rotation around bound C_{14}–C_{15}, almost linear array), giving a more compact hydrophobic core and smaller particles. GC-MIT conjugate with almost twice substitution degree afforded the smaller nanoparticles in solution.

Zeta potential measurements ranged from 18.5 ± 0.6 mV (GC-MST), 36.5 ± 0.6 mV (GC-MIT), 11.7 ± 0.4 mV (GC-MMT) to 36.3 ± 0.9 mV (SCS-MST). These positive zeta potential values are attributed to some positively charged amino groups of chitosan moieties on the surface of nanoparticles (see schematic representation at Fig. 1). Besides mucoadhesive potential and absorption enhancement properties based on electrostatic interactions are expected.

Fig. 7 shows the SEM and TEM images of dried N-tocopheryl glycol chitosan and O6-succinylated chitosan nanoparticles. The SEM images showed almost spherical shaped nanoparticles with 50–100 nm mean diameters. TEM images showed spherical particles with 40–75 nm mean diameters.

In vitro vitamin E release profiles at 37 ± 2 °C in PBS solution (pH 6.0), expressed as per cent cumulative release of DL-α-tocopherol against time from N-tocopheryl glycol chitosans and O6-succinylated chitosan nanoparticles are presented in Fig. 8.

DL-α-Tocopherol was delivered with almost constant release rate (zero order kinetics) during the first 7 h from the N-tocopheryl glycol chitosans and O6-succinylated chitosan nanoparticles. The releases were not quantitative, reaching 49% (GC-MMT), 40% (GC-MST), 30% (SCS-MST) and 24% (GC-MIT), respectively. The bigger GC-MMT nanoparticles with a lower substitution degree and less compact hydrophobic core than the GC-MST particles, released faster the tocopherol; while the smaller nanoparticles of GC-MIT with a very high substitution degree and a more compact tocopheryl hydrophobic core, were less affected by acid hydrolysis and very slowly released tocopherol (see schematic representation in Fig. 1(II)). The selected chitosan derivative also affects the release rate as observed when compared the SCS-MST nanoparticles with the N-tocopheryl glycol chitosan ones. SCS-MST, with the lowest substitution degree and nanoparticles 30 nm smaller than the GC-MIT in PBS solution, released slightly faster than GC-MIT particles.

The antioxidant activities at different time intervals of the tocopheryl-modified self-assembled nanoparticles, expressed as % radical scavenging activity by DPPH test, are shown in Fig. 1(I) of supplementary materials. The antioxidant power in the release medium increased with time in the same way as tocopherol release.

Fig. 1(II) of supplementary materials shows the antioxidant activities of Trolox solutions with molar concentrations adjusted to same concentrations of tocopherol released from nanoparticles.

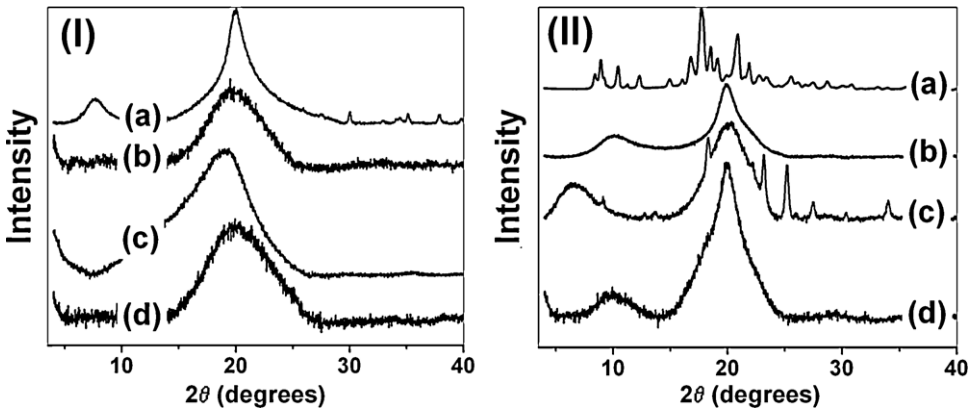

Fig. 5. Wide-angle X-ray diffraction patterns of (I): (a) GC, (b) GC-MST, (c) GC-MIT, (d) GC-MMT; (II): (a) MST, (b) CS, (c) SCS, (d) SCS-MST; (see Fig. 1 for structures).

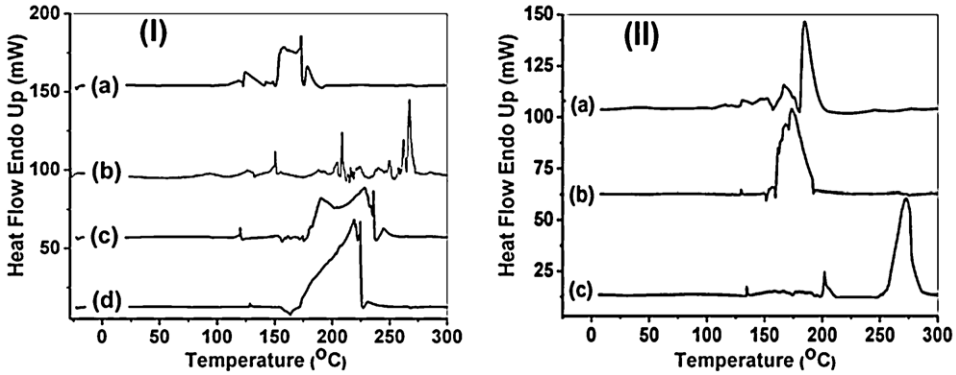

Fig. 6. DSC curves of (I): (a) GC, (b) GC-MST, (c) GC-MIT, (d) GC-MMT; (II) (a) CS, (b) SCS and (c) SCS-MST (see Fig. 1 for structures).

The antioxidant power (measured as radical scavenging activity) of the delivered DL-α-tocopherol (Fig. 1(I) of supplementary materials) was around 80–92% when compared to Trolox solutions (Fig. 1(II) of supplementary materials). Based on these results it can be concluded that the processes carried out during the synthesis of tocopheryl-modified chitosan conjugates, the preparation of the nanoparticles and the release experiments did not affect the antioxidant activity of DL-α-tocopherol.

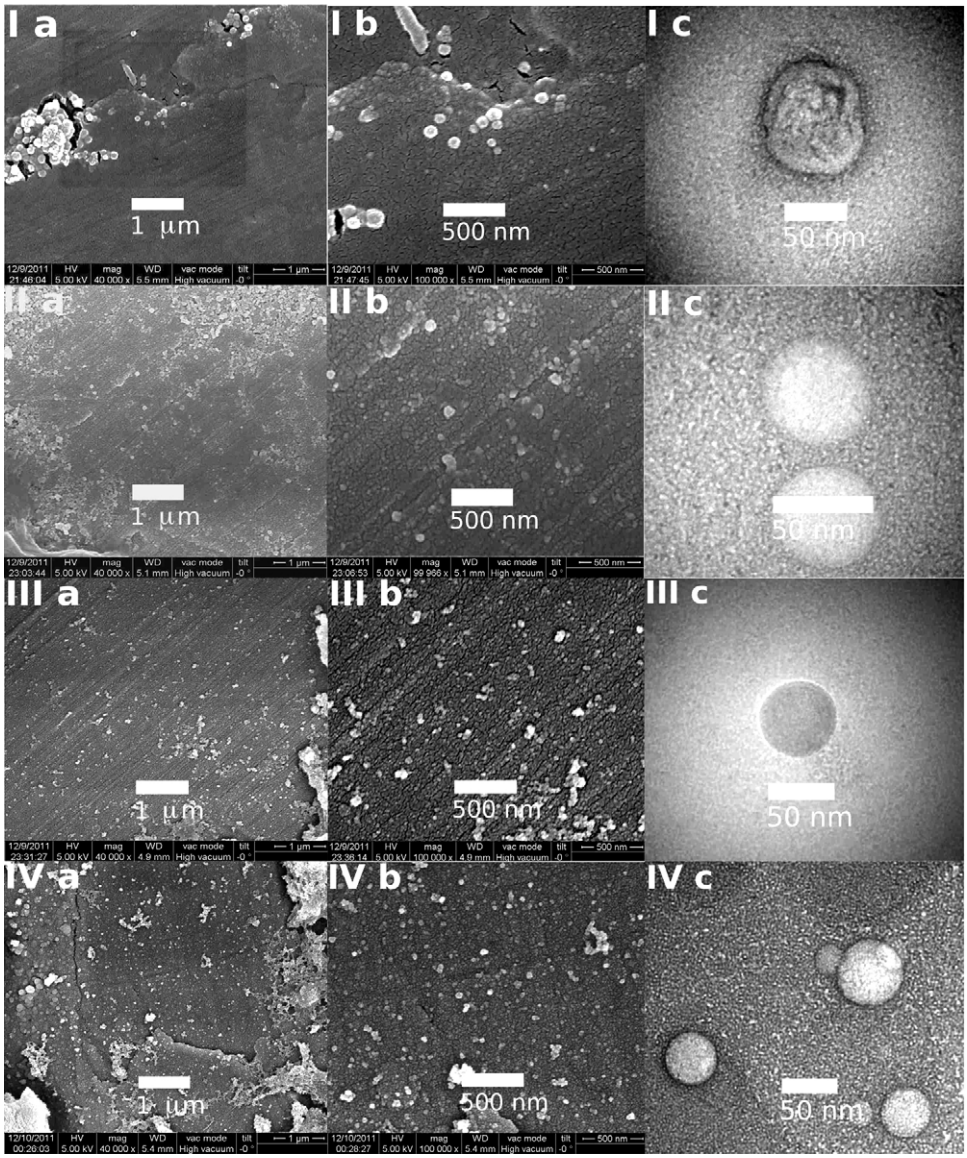

Fig. 7. Scanning electron micrographs of: (I) GC-MST, (II) GC-MIT, (III) GC-MMT and (IV) SCS-MST nanoparticles at (a) 40,000×, (b) 100,000× magnifications and (c) transmission electron micrographs at 100,000× magnifications (see Fig. 1 structures).

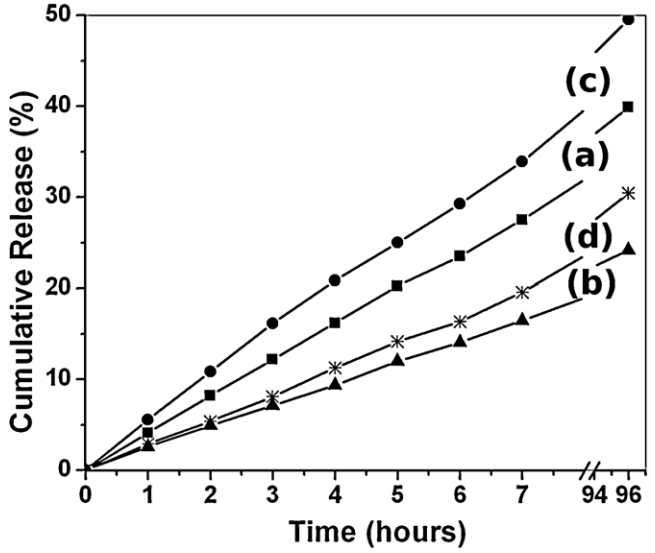

Fig. 8. *In vitro* release profile at 37 ± 2 °C of: (a) GC-MST, (b) GC-MIT, (c) GC-MMT and (d) SCS-MST in phosphate buffered saline solution (pH 6.0) (see Fig. 1 for structures).

Fig. 2(I) of supplementary materials shows the relative cell viability of HMVEC cells at different concentrations of vitamin E (DL-α-tocopherol) and of N-tocopheryl glycol chitosans and N-tocopheryl O6-succinylated chitosan nanoparticles. The HMVEC cell viability is slightly enhanced as a result of treatment with DL-α-tocopherol or with the tocopheryl-modified nanoparticles. These results support the potential application of the studied nanoparticles as a drug delivery system in human and animal health.

Fig. 2(II) of supplementary materials presents the relative cell viability of MCF-7 cells at different concentrations of vitamin E (DL-α-tocopherol) and of N-tocopheryl glycol chitosans and N-tocopheryl O6-succinylated chitosan nanoparticles. The obtained tocopheryl-modified nanoparticles were not cytotoxic to the MCF-7 cell line, as expected of the observed not cytotoxicity of DL-α-tocopherol at the studied concentrations.

4. Conclusions

In this work, some N-tocopheryl O6-succinylated chitosan and glycol chitosan with different substitution degrees were synthesized for controlled release of vitamin E. These tocopheryl-functionalized chitosans were able to form nanoparticles in aqueous solution upon probe tip sonication. The hydrodynamic size in aqueous solution and *in vitro* tocopheryl release rate in acid PBS solution (pH 6.0) and 37 °C of the nanoparticles were affected by tocopherol content and employed chitosan derivative (glycol chitosan or O6-succinylated chitosan). Almost constant release rates were obtained during the first 7 h, but a selection of the linked tocopheryl monoester can result in a faster or slower delivery. The released tocopherol exhibited good antioxidant activity, expressed as radical scavenging activity, when compared to standard Trolox solutions. The potential of these nanoparticles was also demonstrated by the enhancement of HMVEC cell proliferation. The tocopheryl-modified chitosan nanoparticles thus prepared could be potentially applied for controlled release of vitamin E in humans and animals. Besides, the described methodology is suitable to be extended to lipophilic vitamins possessing hydroxyl or carboxyl groups (*i.e.* vitamin A, vitamin D3).

Acknowledgements

The authors wish to thank the Erasmus Mundus Ánimo-Chévere for a research grant to Javier Pérez. Prof. Jacques Chevallier and Ms. Karen E. Thomsen are acknowledged by electron microscopy and staining training at Aarhus University. The Department of Chemistry at University of Paderborn and Ms. Susanne Keuker-Baumman are also acknowledged for elemental analysis and DSC measurements. The authors also wish to thank the Complutense University (Madrid, Spain) and the Santander Group who through their financing of the Program for Distinguished Visitors to Complutense University enabled part of this research work to be carried out.

Appendix A. Supplementary data

Supplementary data associated with this article can be found, in the online version, at http://dx.doi.org/10.1016/j.carbpol.2012.10.005.

References

Abe, T., Hasunuma, K., & Kurokawa, M. (1976). *Vitamin E orotate and a method of producing the same*. US Patent: 3944550.
Acosta, N., Heras, A., & Paños, I. (2008). New drug delivery systems based on chitosan. *Current Drug Discovery Technology*, *5*, 333–341.
Amir, A., Elina, E., Majid, N., Mohammad, A. F., Mohsen, A., & Negar, M.-D. (2010). An Insight into the Interactions between α-tocopherol and chitosan in ultrasound-prepared nanoparticles. *Journal of Nanomaterials*, *2010*, 1–7 [Article ID 818717]
Anraku, M., Fujii, T., Goromaru, T., Hata, T., Kadowaki, D., Kojima, E., et al. (2011). Antioxidant properties of high molecular weight dietary chitosan in vitro and in vivo. *Carbohydrate Polymers*, *83*, 501–505.
Atkinson, J., & Traber, M. G. (2007). Vitamin E, antioxidant and nothing more. *Free Radical Biology and Medicine*, *43*(1), 4–15.
Babak, V. G., Babushkina, T. A., Klimova, T. P., Stepnova, E. A., Tikhonov, V. E., & Vorontsov, E. V. (2007). New approach to the quaternization of chitosan and its amphiphilic derivatives. *European Polymer Journal*, *43*(6), 2414–2421.
Basaran, E., Yazan, Y., & Yenilmez, E. (2010). Release characteristics of vitamin E incorporated chitosan microspheres and in vitro–in vivo evaluation for topical application. *Carbohydrate Polymers*, *84*(2), 807–811.
Berrada, M., Buschmann, M. D., Gupta, A., Lavertu, M., Rodrigues, A., Serreqi, A. N., et al. (2003). A validated ^{1}H NMR method for the determination of the degree of deacetylation of chitosan. *Journal of Pharmaceutical and Biomedical Analysis*, *32*, 1149–1158.
Bongiorno, D., Ceraulo, L., Ferrugia, M., Filizzola, F., Longo, A., & Mele, A. (2006). Interactions of α-tocopherol with biomembrane models: Binding to dry lecithin reversed micelles. *International Journal of Pharmacy*, *312*, 96–104.
Brigelius-Flohé, R., & Traber, M. G. (1999). Vitamin E: Function and metabolism. *The FASEB Journal*, *13*(10), 1145–1155.
Buring, J. E., Glynn, R. J., Goldhaber, S. Z., Ridker, P. M., & Zee, R. Y. (2007). Effects of random allocation to vitamin E supplementation on the occurrence of venous thromboembolism: Report from the Women's Health Study. *Circulation*, *116*(13), 1497–1503.
Cho, Y. W., Chung, H., Jeong, S. Y., Kim, K., Park, J. H., & Son, Y. J. (2006). Preparation and characterization of self-assembled nanoparticles based on glycol chitosan bearing Adriamycin. *Colloid Polymer Science*, *284*(7), 763–770.
Christen, S., Jiang, Q., & Reiter, E. (2007). Anti-inflammatory properties of α- and γ-tocopherol. *Molecular Aspects of Medicine*, *28*(5–6), 668–691.
David, L., Domard, A., Lucas, J.-M., Osorio-Madrazo, A., Peniche-Covas, C., & Trombotto, S. (2010). Kinetics study of the solid-state acid hydrolysis of chitosan: Evolution of the crystallinity and macromolecular structure. *Biomacromolecules*, *11*, 1376–1386.
Duclairoir, C. (2002). α-Tocopherol encapsulation and in vitro release from wheat gliadin nanoparticles. *Journal of Microencapsulation*, *19*(1), 53–60.
Fang, Y., & Huang, M. (2006). Facile preparation of biodegradable chitosan derivative having poly(butylene glycol adipate) side chains. *Biopolymers*, *82*, 597–602.
Gray, A. I., Mahmoud, A., Sadiq, L., Schätzleinä, A. G., Uchegbu, I. F., Waigh, R. D., et al. (2001). Quaternary ammonium palmitoyl glycol chitosan—a new polysoap for drug delivery. *International Journal of Pharmaceutics*, *224*, 185–199.
Gray, A. I., Noble, L., Sadiq, L., & Uchegbu, I. F. (1999). A non-covalently cross-linked chitosan based hydrogel. *International Journal of Pharmaceutics*, *192*, 173–182.
Hirai, A., Nakajima, A., & Odani, H. (1991). Determination of degree of deacetylation of chitosan by ^{1}H NMR spectroscopy. *Polymer Bulletin*, *26*, 87–94.
Jing-Mou, Y., Li-Yan, Q., Yi, J., & Yong-Jie, L. (2008). Self-aggregated nanoparticles of cholesterol-modified glycol chitosan conjugate: Preparation, characterization, and preliminary assessment as a new drug delivery carrier. *European Polymer Journal*, *44*, 555–565.
Kean, T., & Thanou, M. (2010). Biodegradation, biodistribution and toxicity of chitosan. *Advanced Drug Delivery Reviews*, *62*, 3–11.

Liu, N., & Park, H.-J. (2009). Chitosan-coated nanoliposome as vitamin E carrier. *Journal of Microencapsulation*, *26*(3), 235–242.
Lodge, J. K. (2005). Vitamin E bioavailability in humans. *Journal of Plant Physiology*, *162*(7), 790–796.
Mau, J.-L., Yang, J., & Yen, M.-T. (2009). Physicochemical characterization of chitin and chitosan from crab shells. *Carbohydrate Polymers*, *75*, 15–21.
Muzzarelli, R. A. A. (2009). Chitins and chitosans for the repair of wounded skin, nerve, cartilage and bone. *Carbohydrate Polymers*, *76*(2), 167–182.
Muzzarelli, R. A. A., Boudrant, J., Meyer, D., Manno, N., De Marchis, M., & Paoletti, M. G. (2012). Current views on fungal chitin/chitosan, human chitinases, food preservation, glucans, pectins and inulin: A tribute to Henri Braconnot, precursor of the carbohydrate polymers science, on the chitin bicentennial. *Carbohydrate Polymers*, *87*, 995–1012.
Quiñones, J. P., Coll, Y., Curiel, H., & Covas, C. P. (2010). Microspheres of chitosan for controlled delivery of brassinosteroids with biological activity as agrochemicals. *Carbohydrate Polymers*, *80*(3), 915–921.
Quiñones, J. P., Gothelf, K. V., Kjems, J., Caballero, A. M. H., Schmidt, C., & Covas, C. P. (2012). Self-assembled nanoparticles of glycol chitosan – ergocalciferol succinate conjugate, for controlled release. *Carbohydrate Polymers*, *88*, 1373–1377.
Ravi Kumar, M. N. V., Muzzarelli, R. A. A., Muzzarelli, C., Sashiwa, H., & Domb, A. J. (2004). Chitosan chemistry and pharmaceutical perspectives. *Chemical Reviews*, *104*, 6017–6084.
Shen, J., Ping, Q., Zhang, C., & Zhang, H. (2003). Synthesis and characterization of water-soluble O-succinyl-chitosan. *European Polymer Journal*, *39*, 1629–1634.